Title

Posttranscriptional Regulation of Gcr1 Expression and Activity Is Crucial for Metabolic Adjustment in Response to Glucose Availability

Journal

Molecular Cell, 62(3)

ISSN

1097-2765

Authors

Hossain, Munshi Azad
Claggett, Julia M
Edwards, Samantha R
et al.

Publication Date

2016-05-01

DOI

10.1016/j.molcel.2016.04.012

Peer reviewed

HHS Public Access

Author manuscript

Mol Cell. Author manuscript; available in PMC 2017 May 05.

Published in final edited form as:

Mol Cell. 2016 May 5; 62(3): 346–358. doi:10.1016/j.molcel.2016.04.012.

Post-transcriptional regulation of Gcr1 expression and activity are crucial for metabolic adjustment in response to glucose availability

Munshi Azad Hossain[§], **Julia M. Claggett**[§], **Samantha Edwards**, **Aishan Shi**, **Sara Pennebaker**, **Melodyanne Cheng**, **Jeff Hasty**[‡], and **Tracy L. Johnson**[*]

Molecular Cell and Developmental Biology, Terasaki Life Sciences Building Room 5159, 610 Charles Young Dr. E, Los Angeles, CA 90095-7239, Phone: (310) 206-2416

Summary

The transcription factor Gcr1 controls expression of over 75% of the genes in actively growing yeast. Yet, despite its widespread effects, regulation of Gcr1 itself remains poorly understood. Here we show that posttranscriptional Gcr1 regulation is nutrient-dependent. Moreover, *GCR1* RNA contains a long, highly conserved intron, which allows the cell to generate multiple RNA and protein isoforms whose levels change upon glucose depletion. Intriguingly, an isoform generated by intron retention is exported from the nucleus, and its translation is initiated from a conserved, intronic translation start site. Expression of gene products from both the spliced and unspliced RNAs is essential, as cells expressing only one isoform cannot adjust their metabolic program in response to environmental changes. Finally, we show that the Gcr1 proteins form dimers, providing an elegant mechanism by which this one gene, through its regulation, can perform the repertoire of transcriptional activities necessary for fine-tuned environmental response.

eTOC blurb

Hossain, Claggett *et al.* demonstrate that expression of the critical glycolytic transcription factor Gcr1 is regulated at multiple levels, including intron-retention and utilization of intronic translation signals, to allow cells to adjust their metabolic program in response to glucose availability.

[*]Correspondence: tljohnson@ucla.edu.

[§]Co-first author.

[‡]San Diego Center for Systems Biology, Molecular Biology Section, Division of Biological Sciences, University of California, San Diego, CA, 92093, USA

Author Contributions: Experimental Design, M.A.H., J.M.C., and T.L.J.; Formal Analysis, M.A.H. and T.L.J.; Investigation, M.A.H., J.M.C., S.E., A.S., S.P., M.C.; Conceptualization, J.M.C., M.A.H. and T.L.J.; Visualization, M.A.H. and T.L.J.; Writing-Original Draft, J.M.C. and T.L.J.; Writing-Revised Draft, M.A.H. and T.L.J.; Writing–Review & Editing, M.A.H., S.E., and T.L.J.; Funding Acquisition, T.L.J. and J.H.; Supervision, T.L.J.

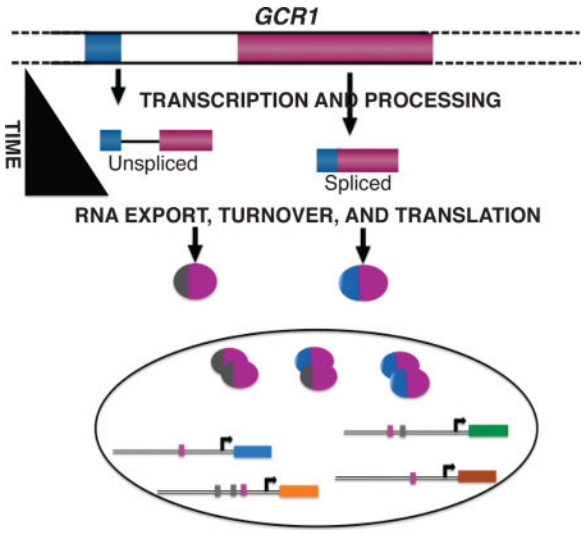

Introduction

In a dynamic environment, cells undergo precise metabolic changes that are determined by tightly regulated gene expression reactions. This is particularly important for single-celled organisms, such as *Saccharomyces cerevisiae*, since a failure in this fine-tuning can directly affect the viability of the organism. Although the majority of yeast studies are performed on actively dividing cells in a nutrient-rich environment, there is an increasing interest in understanding how cells respond to nutrient deprivation. In the absence of nutrients, such as glucose, both yeast and mammalian cells assume a state of quiescence (Longo and Fabrizio, 2002). The ability (or inability) to establish and maintain quiescence in human cells is important for stem cell maintenance, wound healing, and, of course, cancer (Gray et al., 2004).

Yeast cells metabolize glucose through the process of glycolysis, leading to exponential cell division. As glucose is exhausted from the media, cells undergo diauxic shift, and this rapid growth ceases as cells adjust their metabolic pathways to use the byproducts of glycolysis to generate storage carbohydrates. While it is clear that the cellular response to glucose depletion occurs through widespread changes in gene expression, the molecular mechanisms underlying these changes are not fully understood.

The transcription factors responsible for co-regulating the expression of the enzymes in the glycolytic/gluconeogenic pathway have largely been identified (Chambers et al., 1995), and one such transcription factor is Gcr1 (Glycolysis Regulator 1). However, while Gcr1 influences the production of over 75% of all RNA Polymerase II transcripts in actively growing yeast (Warner, 1999), the mechanisms by which Gcr1 regulates glycolytic gene expression in response to glucose availability remain largely unknown. Furthermore, there are many unanswered questions about how Gcr1 is itself regulated. For example, *GCR1* contains an intron, but the relative contributions of *GCR1* splicing and intron retention to the regulated expression of the Gcr1 protein have not been explored. Nor is it clear whether retention of the *GCR1* intron contributes to Gcr1 function, even though in recent years intron

retention has been implicated as an important mode of splicing regulation in *S. cerevisiae* and other eukaryotes (Johnson and Vilardell, 2012). The regulation of Gcr1 expression and activity remains a critical question in light of the profound effect that Gcr1 has on the gene expression program of the cell.

Here we examine Gcr1 function and show that it is regulated in response to glucose availability, and this regulation is central to glycolytic gene expression and cellular metabolism. Gcr1 protein decreases to nearly undetectable levels after cells have depleted glucose from the media, indicating tight control on Gcr1 protein expression. An examination of the *GCR1* RNA reveals that in the presence of glucose, multiple isoforms are generated via alternative splicing, use of an alternative transcription start site, and RNA decay. One of these isoforms is the product of *GCR1* intron retention. Surprisingly, this product contains an intronic start codon that permits translation of a protein isoform with the same C-terminal DNA binding domain as the Gcr1 protein derived from the spliced transcript, but the two proteins have different N-terminal activation domains. While all of the RNA and protein isoforms decrease as cells enter stationary phase, they do so with different rates, suggesting that the ratios of these isoforms are important for cell adaptation. Detailed analysis of cells transitioning into stationary phase reveals that optimal expression of *Gcr1* target genes involved in glycolysis, gluconeogenesis, and the transition between metabolic states is absolutely dependent upon expression of these different isoforms. Finally, we show that each of the Gcr1 protein isoforms homo- and heterodimerize, thus generating a repertoire of Gcr1 transcription factors and providing a rationale for why cells perform optimally only when they possess the ability to alternatively process *GCR1*. These findings not only identify new isoforms of Gcr1—arguably one of the most important metabolic transcription factors in yeast—but also provide a striking example of how alternative splicing in the form of intron-retention can present the cell with novel mechanisms for regulating gene expression.

Results

Gcr1 protein levels decrease when glucose is depleted

In light of the critical and widespread effects of Gcr1 on gene expression, we were interested in understanding its regulation. A significant number of the genes that are positively regulated by Gcr1 are involved in glucose metabolism (Lopez and Baker, 2000; Sasaki and Uemura, 2005), suggesting that Gcr1p levels may be negatively regulated during growth into stationary phase, when the glycolytic demands of the cell decrease, to mediate a metabolic shift in response to glucose depletion. To test this, cells containing a tagged version of Gcr1 were grown in rich media, and Gcr1 protein levels were analyzed relative to total protein over time, which was measured and validated by electrophoresis and protein staining (Figure S1A). Gcr1 migrated between 100–135 kDa, corresponding to the expected molecular weight of 109kDa (total size includes the tag). Moreover Gcr1 levels decrease dramatically between 6 and 8 hrs and remain low (Figure 1A). To correlate the decrease in Gcr1 levels with the metabolic state of the cell, we analyzed both cell growth and the concentration of extracellular glucose. The rapid drop in Gcr1p levels consistently occurs as cells approach diauxic shift (OD ~2.8) (Gray et al., 2004), and total Gcr1 levels become nearly undetectable post-diauxic shift. A representative example of these results is shown in Figure 1A, lower

panel. We noted that a doublet was clearly visible by western during this time course, and since there were previous reports of Gcr1 phosphorylation (Zeng et al., 1997), the samples were treated with phosphatase (Figure S1B). Although the bands were sharpened in the presence of phosphatase, the doublet was apparent even after the treatment.

Cells lacking Gcr1 misregulate accumulation of storage carbohydrates

Yeast cells entering stationary phase undergo dramatic reprogramming that reduces the efficiency of glycolysis, enables them to adjust their metabolism to changing carbon sources, and eventually allows cells to survive during starvation (DeRisi et al., 1997; Gasch et al., 2000). If downregulation of Gcr1 were necessary for this reprogramming, one would expect *GCR1* to be dispensable for growth on non-fermentable carbon sources. Indeed, similar to what has been previously documented for a mutant allele of *GCR1* (*gcr1-6*; (Uemura and Fraenkel, 1990)), cells deleted of *GCR1* show impaired growth on fermentable carbon sources, and growth comparable to WT on non-fermentable carbon sources (Data not shown).

Since cells deleted of *GCR1* appear to behave like WT cells post-diauxic shift during which the gluconeogenic pathway is triggered, we rationalized that *gcr1*Δ cells would prematurely show gluconeogenic signatures. To address this, we assessed the levels of storage carbohydrates (such as trehalose and glycogen) in *gcr1*Δ cells relative to WT cells. Consistent with our hypothesis, the levels of trehalose were higher in *gcr1*Δ cells (120μg/ml) than in WT cells during exponential growth (Figure 1B). In fact, the level of trehalose in *gcr1*Δ cells during exponential growth was nearly equivalent to that of WT cells post-diauxic shift (130 μg/ml at 12 hrs), when Gcr1p levels are undetectable by western analysis in a WT strain (Figure 1A). The above trend was also observed for *gcr1*Δ relative to WT with respect to glycogen (Figure 1C), as we observe a significant increase in the level of glycogen in *gcr1*Δ cells compared to WT cells (600 mg/ml vs. 90 mg/ml, respectively) during early post-diauxic shift. This finding demonstrates that the lack of Gcr1 leads to changes in gene expression that result in unregulated accumulation of storage carbohydrates. It also suggests that downregulation of Gcr1 during diauxic shift contributes to critical changes in gene expression that enable the cell to synthesize and utilize storage carbohydrates.

GCR1 has unique features that suggest regulated RNA processing

GCR1 contains an intron that was shown to be inefficiently spliced (Tornow and Santangelo, 1994), although the relative amounts of spliced versus unspliced *GCR1* RNA have not been examined. Intriguingly, the *GCR1* intron has a number of unusual features. While the mean intron length in yeast is 264 nucleotides (n=198; (Bon et al., 2003)), the *GCR1* intron is exceptionally long, 739 nucleotides, and contains the rare 5′SS sequence GUAUG**A**, found in only nine other intron-containing genes in *S. cerevisiae* (Figure 2A). This non-canonical 5′SS sequence is conserved across the *Saccharomyces* species most closely related to *S. cerevisiae* (*S. paradoxus, S. mikatae, S. kudriavzevii, S. bayanus*, and *S. pastorianus*) suggesting that it may play an important role in determining how *GCR1* splicing might be regulated. Our own previous studies of another RNA with this non-canonical 5′SS showed that this sequence contributes to intron retention (Hossain et al., 2011). The high degree of

conservation for this unusual 5′SS sequence prompted us to examine the splicing of *GCR1* more closely.

Different *GCR1* isoforms are produced via splicing

In order to determine whether alternative processing of *GCR1* contributes to its regulation, we analyzed total RNA from a WT strain by northern blot using a probe for the second exon of *GCR1* (Figure 2A). As a control to show where unspliced RNA migrates, we generated a *GCR1* construct with a mutation at the branchpoint (A → G), which prevented the RNA from being spliced (Figure 2B, lane 1). Although previous studies and the presence of the non-canonical splice site suggested that *GCR1* intron removal might be inefficient, we were surprised to find that, at early timepoints, the majority of *GCR1* RNA appears to be unspliced (Figure 2B, 0 hr). The WT strain was allowed to grow continuously and total RNA was analyzed at 2 hr intervals to determine whether the *GCR1* RNA changed over time, particularly in light of the rapid decrease in Gcr1p levels after 6 hrs, and indeed, total *GCR1* RNA also decreased over time (Figure 2B). Interestingly, the ratio of the unspliced and a faster migrating species that we suspected to be the spliced RNA also changed over time. During early timepoints (0–4 hrs), there was greater accumulation of unspliced products (~60% of total RNA), and around the diauxic shift we observed a relatively greater accumulation of spliced product (65–55% of total RNA) (Figure 2B, right hand panel). Interestingly, an even smaller transcript was detectable at these later timepoints (6–12 hrs). These data suggest that *GCR1* expression is regulated at the RNA level during glucose depletion. The RNA samples are run to allow *SCR1* to be retained in the gel. Moreover, the bands that we detect with the radioactive probe run coincident with the rRNA. Both of these considerations influence the separation of the bands. So even though all gels are run with size markers, we sought to assess their identities more precisely.

In order to further evaluate the identities of the RNAs detected by northern blot, we performed “probe-walking” northern using probes that annealed to different regions of *GCR1* using the RNA samples collected at the 6- and 8-hr timepoints from WT cells and *gcr1*Δ cells (Figure 2C). Each northern strip containing a marker and RNA from *gcr1*Δ cells and WT cells was aligned after hybridization to determine the relative mobility of the hybridized bands (see Supplemental Experimental Procedures for details). The radioactive probes spanning Exon 2—from the 3′ end (Ex2.4 probe) to the 5′ end (Ex2.1 probe) annealed to both the unspliced and the faster migrating (“spliced”) product (Figure 2C). However, the In1 probe hybridized to only one of the bands (Figure 2C, lanes 17 and 18). Furthermore, alignment of the In1 blot and the blot probed with the Ex2.2 probe (which were transferred from the same gel, Figure S2A) indicates that the unique band corresponds to the unspliced RNA, and the In1 probe did not hybridize to “spliced” RNA products, consistent with intron removal; nor did it anneal to the smaller RNA product (Figure 2C, lanes 17 and 18, S2A). A probe spanning from the 5′UTR and Exon1 to the intronic sequences just downstream of the Exon1 (UTR-Ex1.In) annealed to both the unspliced and the spliced isoform (Figure 2C, Table S1 for primer sequences), consistent with the presence of the 5′UTR and exon1 in both of these RNAs. We consistently observe less hybridization signal for the spliced products than the unspliced isoform using this probe even though the spliced RNA also contains exon1 and the 5′UTR sequence (Figure 2C, lanes 20 and 21).

This is not surprising since the spliced products lack the intronic sequence, whereas, the unspliced isoform with the retained intron allows greater hybridization with the UTR-Ex1.In probe. Importantly, the ability of the probe to anneal to both of these RNA species reinforces our identification of spliced isoforms and further indicates that the spliced products contain the Exon1 and 5′UTR sequences.

The small RNA product is comprised of the second exon

We next focused our attention on the smaller RNA product that migrates with a faster mobility than the "spliced" RNA. Neither the intronic probe (In1), nor the 5′ exon probe (UTR-Ex1.In) annealed to this RNA. Furthermore, this product efficiently hybridized to all of the Exon2 probes except Ex2.1, at the very 5′ end of the exon. Since the Ex2.2 probe annealed, while the 2.1 probe did not, we tested annealing of another probe, Ex2.1-2, which hybridized between Ex2.2 and Ex2.1, (Figure 2C, fourth panel). These experiments suggested that the smaller product contains most of Exon2 and initiates near the 5′ end of Exon2. In order to precisely identify the 5′ end of the smaller transcript(s), we performed 5′RACE with RNA samples from the 6-hr timepoint using an Exon2 primer. Consistent with the northern analysis, the sequence of the cloned RACE products terminates in the region of the Ex2.1.2 probe (Figure S2B). Taken together, these results indicate that around the time of the diauxic shift (between 6–8 hrs), an RNA comprised largely of the second exon is generated. Interestingly, we also detect this RNA product in cells expressing nsDNA. At the 6- and 8 hr timepoints, when the "spliced" RNA and the smaller transcripts are most abundant in WT cells (Figure 2B), no spliced RNA is detected, while the smaller product is clearly visible (Figure S2C lanes 3 and 4). The fact that we do not detect spliced product in cells expressing nsDNA, suggests that the smaller RNA product is not generated through splicing but likely through transcription that initiates from within the intron (Figure S2C). To be sure that the smaller RNAs were generated from the same strand as the unspliced RNA, we used strand-specific probes (Figure S2D) for northern analysis. The results confirmed that the small transcripts were generated from the same strand as the *GCR1* unspliced transcript.

GCR1 generates multiple spliced isoforms

We consistently observed that the band represented by the spliced RNA appeared as a thicker "smear," compared to the unspliced band, leading us to wonder whether the "spliced" *GCR1* isoform might also represent multiple products. To address this, RT-PCR was performed using primers flanking the intron and potential 5′ and 3′ splice sites. Each band was extracted from the gel and sequenced to reveal that 8 *GCR1* spliced isoforms are produced by the alternative use of three possible 5′SSs and four 3′SSs (Figures 2D and S3A). During the course of our study Kawashima *et al.* also determined by RNA sequencing that *GCR1* generates multiple isoforms (Kawashima et al., 2014), confirming the complex splicing capability of *GCR1.* Interestingly, only two of the spliced isoforms generate in-frame proteins from the AUG in the first exon (see asterisks in figure 2D); the other 6 isoforms that we detected contain a premature termination codon (PTC). Relative to the other in-frame isoform, the annotated spliced isoform is found in low abundance, suggesting that the actual spliced isoform that encodes the Gcr1 protein is not the annotated form of the RNA but the newly-identified, in-frame spliced species. Differences in the relative amounts

of these isoforms can account for the slight variation in "spliced" band mobility observed in the northerns. We also performed RT-PCR to examine whether cells expressing nsDNA generate any spliced isoforms (Figure S2F). Consistent with our northern data (Figure S2C), no spliced RNA is detected, indicating that a single branchpoint is used to generate the isoforms (Figure S3B).

GCR1 transcripts are targets of the RNA decay machinery

Studies of yeast genes with regulated intron retention have demonstrated that, under regulatory conditions, many of these intron-containing RNAs are exported from the nucleus and targeted for nonsense-mediated decay (NMD) (reviewed by (Johnson and Vilardell, 2012)). NMD targets transcripts with a premature termination codon (PTC). The only other elements found to correlate with targeted RNA decay by Upf1 (the primary component of the NMD machinery) or Xrn1 (the major 5′-3′ exonuclease that acts in concert with NMD) are suboptimal splice site sequences; specifically, a suboptimal 5′SS or branchpoint appears in nearly half of all NMD-sensitive introns (Sayani et al., 2008). Since the intron of *GCR1* contains both a PTC and a suboptimal 5′SS, we hypothesized that unspliced *GCR1* might also be subject to regulation by cytoplasmic decay. We measured the levels of *GCR1* RNA over 12 hrs in cells deleted of either *XRN1* or *UPF1*. Indeed, the level of unspliced *GCR1* transcript is higher in strains deleted of either *UPF1* or *XRN1* compared to WT (Figures 2E and S4). However, *XRN1* had a much greater effect than *UPF1* at all timepoints until about 12 hrs when the levels of all isoforms are low (Figure 2E). Xrn1 is found in a number of cytoplasmic foci such as stress granules and P-bodies, which have been shown to form as glucose is depleted from the growth medium, and are present throughout both the post-diauxic shift and stationary phases of growth (Shah et al., 2013). It is possible that *GCR1* RNAs localize to these dynamic foci to allow for their regulation and release when the glucose conditions are appropriate. Interestingly, cells deleted of *or* overexpressing *XRN1* show a decreased vegetative growth rate (Yoshikawa et al., 2011) data not shown).

The spliced and intron-containing *GCR1* transcripts are translated to produce different Gcr1p isoforms

The presence of the retained intron suggested to us that there might be functional consequences to intron retention. We also noted two in-frame start codons within the intron, and translation from either would generate an in-frame protein of a similar molecular weight as the protein predicted from spliced *GCR1* mRNA (116 vs. 109 kDa with the TAP tag). Despite the similarity in size, differential use of the Exon1 translation start site versus the intronic translation start site would lead to a 62 amino acid difference in the sequence at the N-terminus of the protein. Notably, the location of the first ATG within the intron and the intronic sequence downstream of this ATG is nearly identical (86%–99%) among the five closely-related *Saccharomyces* species (Figure 3A), suggesting that translation of the intron-containing *GCR1* transcript may be of biological importance to the cell.

To test whether a protein is generated from unspliced *GCR1*, the *GCR1* nsDNA construct was expressed in a *gcr1*Δ strain. This was compared to strains expressing either the genomic DNA (gDNA) with the intron or the cDNA from the spliced product (cDNA). As shown in Figure S5A, the gDNA expression from plasmid behaves nearly identically to chromosomal

GCR1. Strikingly, the unspliced RNA can be translated, as the nsDNA generates a stable protein product detectable by western (Figure 3B, lane 3). We compared the mobility of this protein to the proteins detected when the cells express the gDNA or cDNA (Figure 3B). As expected, the Gcr1 protein expressed from gDNA shows two bands, one that corresponds to the cDNA derived protein and the other that corresponds to the nsDNA derived protein.

The ATGs within the intron are utilized to generate Gcr1 protein

We next wanted to understand how Gcr1 protein was produced from the unspliced RNA. In order to address this, we generated a construct (int-*GCR1*) containing the intronic ATGs. The 5′ region of the intron, Exon1, and the 5′UTR sequences were excluded to avoid any confounding effects (Figure 3C). We also generated a construct in which both the ATGs were mutated to AAG (intmATGs-*GCR1*) (Figure 3C). The protein products from these constructs were analyzed by western blot to reveal that the int-*GCR1* construct expresses a protein of the same size as the protein expressed from nsDNA (Figure 3C, lanes 3 and 4), whereas the intmATGs-*GCR1* construct does not express any protein (Figure 3C, lane 5). Both the proteins expressed from the nsDNA and the int-*GCR1* migrate with the same mobility as the higher molecular weight protein from the gDNA. Moreover, the cells expressing these constructs grow indistinguishably (Figure S5B), which also validates that the mutation at the BP, per se (Asn to Ser) does not significantly change the function of the protein produced from the unspliced RNA. In order to assess whether expression of the protein is important for cell viability, we analyzed the growth of the *gcr1*Δ cells harboring either the int-*GCR1* or the intmATGs-*GCR1* constructs and found that the intmATGs-*GCR1* show a severe growth defect, identical to *gcr1*Δ, while int-*GCR1* cells grow well (Figure 3D). These data confirm that the intronic ATGs are used to translate a protein that is important for cell growth on glucose-containing media.

To further analyze the utilization of the ATGs in *GCR1*, we generated the construct gDNA-intmATGs, in which both intronic ATGs were mutated, while the Exon1 ATG remained intact (Figure 3E). We hypothesized that upon splicing of the *GCR1* transcript, the spliced isoform would generate a protein, but protein would not be translated from the unspliced transcript with the intronic ATGs mutated. Indeed, we observe expression of a protein with the same mobility as the protein expressed from cDNA (Figure 3E, lanes 3 and 4). Protein expressed from a construct in which the Exon1 ATG was mutated to AAG, but the intronic ATGs were left unchanged migrates with a mobility that matches the nsDNA-derived protein and not with the cDNA (Data not shown). We sometimes observe slightly smeared migration of the specific Gcr1p isoforms (Figures 3C and 3E), which is most likely due to Gcr1p phosphorylation (Zeng et al., 1997).

Together these data indicate that the *GCR1* transcript can make multiple Gcr1p isoforms—one from the cDNA and another isoform that is translated from the unspliced transcript using the intronic ATGs. Moreover this product is functional (Figure 3D). This is particularly interesting in light of the fact that the ribosome appears to recognize this sequence in the unspliced RNA despite the presence of the start codon in the Exon1, which would be encountered first by a scanning ribosome. Use of this AUG would also be expected to trigger NMD since there is an intronic PTC just downstream of it. However, we find that

not only does the unspliced RNA largely escape the *UPF1*-dependent NMD pathway at almost all timpoints measured (Figure 2E), but also the downstream translation start site in the intron is very efficiently utilized.

Previous studies of Gcr1 derived from cDNA have defined the domains of the protein. The Gcr1 cDNA-derived protein has a DNA binding domain in the C-terminus (codons 631-785; (Huie et al., 1992)), and an activation domain in the N-terminus (codons 7-306; (Tornow et al., 1993)), all of which lie *downstream* of the 3′ splice site. N-terminal truncation mutants (codons 11-211) were unable to complement the *gcr1*Δ growth defect (Tornow et al., 1993). The protein generated from the unspliced *GCR1* transcript encodes 62 amino acids of unique sequence at the N-terminus, a part of the protein known to be important for modulating Gcr1 transcriptional activity.

We were intrigued by the possibility that the RNA comprised of the Exon2 might generate a protein as well, particularly because there are in-frame ATGs at the 5′ end of this transcript. Since, northern analysis showed that this RNA is generated at the time when *GCR1* expression goes down (Figure 2B), we even considered the possibility that a protein derived from this RNA might negatively regulate expression of *GCR1*. However, we have been unable to detect a protein product in this range from either the endogenous *GCR1* gene, the gDNA, nsDNA, cDNA, or other mutant constructs, even when we focused on proteins isolated between 6–10 hrs, when the Exon2 RNA is first detected (data not shown). It is possible that a protein is made but is either extremely unstable or translated at low levels. It is also possible that the RNA itself or simply its synthesis has some function, perhaps in *GCR1* autoregulation. At present, we cannot distinguish between these models. As such, we have focused on understanding the functions of the unexpected proteins that are clearly distinguishable by western and appear to play essential roles in the metabolic adjustment of cells. Studies to understand the Exon2 RNA product are ongoing.

Exclusive expression of the *GCR1* cDNA or nsDNA isoform leads to impaired growth and gene expression

In light of our observation that two Gcr1 protein isoforms are produced, we wanted to determine how expression of individual isoforms affects cells growing in glucose and as they transition to nutrient-depleted conditions. We expressed *GCR1* gDNA, nsDNA, cDNA, or empty vector in *gcr1*Δ cells and compared this to WT cells grown in liquid batch media. *Gcr1*Δ cells expressing *GCR1* gDNA grow nearly identically to WT cells, indicating that all isoforms necessary for optimal growth are produced from this construct. As expected, *gcr1*Δ cells grow extremely poorly. The *gcr1*Δ cells expressing nsDNA or cDNA grow more slowly than gDNA expressing cells. In fact, the overall growth rate of *GCR1* nsDNA and *GCR1* cDNA is 1.5–2 fold slower between 6 and 24 hrs compared to *GCR1* gDNA (Figure 4A).

Efficient glucose metabolism is a highly regulated process that depends on the coordinated regulation of highly expressed glycolytic genes. In order to examine the impact of the *GCR1* isoforms on glycolytic gene expression, we analyzed the expression of a number of well-characterized Gcr1-target genes that are involved in the glycolytic pathway—specifically, *TPI1, ENO2, PYK1, ADH1* (Huie et al., 1992). Interestingly, like many glycolytic genes, these genes also contain binding sites for other transacting factors: Rap1, Reb1 and Abf1.

We also analyzed genes (*GLK1* and *HXK1*), which are not direct targets of Gcr1 but show impaired expression in a *gcr1*Δ strain (Sasaki and Uemura, 2005). Finally, since the metabolic state of the cell is altered by the activities of Gcr1 targets that affect synthesis and utilization of storage carbohydrates, we also analyzed the expression of genes involved in trehalose (*TPS2*) and glycogen (*GLC3*, *GSY1*, *GDB1*) biosynthesis.

Our analysis reveals dramatic de-regulation of all of the genes queried upon exclusive expression of the nsDNA or cDNA compared to the gDNA. For example, *ENO2* shows 2-fold higher expression in cells expressing cDNA compared to gDNA at 6 hrs, and the expression remains high until 10 hrs (Figure 4B). On the other hand, for cells expressing nsDNA, *ENO2* expression remains low at the 4- and 6-hr timepoints and then rises at the 10 hr timepoint compared to gDNA (Figure 4B). Notably, deletion of *GCR1* abolishes the expression of *ENO2* altogether (Figure 4B, dotted line). It is also interesting that in the case of *ENO2*, the two isoforms have the opposite effect at particular timepoints, neither of which is the WT level of expression.

As we observed significant differences for *ENO2* expression at the 6hr timepoint, we determined the total amount of Gcr1p expressing from gDNA, cDNA and nsDNA at this timepoint. It is important to note that all of the *GCR1* constructs were under the control of the native *GCR1* promoter and were expressed from the identical plasmid in order to ensure that the levels of Gcr1p were comparable. All the constructs express comparable levels of total Gcr1p; with the nsDNA-derived protein showing slightly higher levels (Figure 4C), indicating that the relative levels of the isoforms cannot alone explain the differences in expression of *ENO2*. We then analyzed the expression of other Gcr1 target genes. Cells expressing either nsDNA or cDNA show altered expression of glycolytic genes compared to the expression of gDNA. Notably, although gDNA and cDNA express equivalent amounts of total Gcr1p, we observed significantly impaired gene expression in cells expressing cDNA (Figure 4C, bar graph). Moreover, higher level expression of Gcr1p from the nsDNA did not result in increased expression of Gcr1 target genes compared to cDNA. In fact, in some cases, expression of nsDNA results in lower expression of the Gcr1 target gene relative to gDNA (Figures 4C and 4B). We further analyzed gene expression and Gcr1p levels at other timepoints in cells expressing the gDNA, cDNA, and nsDNA (Figures 4D). In most cases, sole expression of cDNA leads to overexpression of genes tested at the 2 hr and 4 hr time points. At the 10hr timepoint both nsDNA and cDNA result in overexpression of genes although the cDNA effect is often greater (Figure 4D). Despite the differences in gene expression, we observe similar levels of protein from gDNA and cDNA, with slightly higher protein expression from the nsDNA (Figure S6). Overall, temporal control of gene expression diverged, sometimes dramatically, from gDNA when either nsDNA or cDNA was expressed exclusively (Figure 4D). Hence, it is clear that the glycolytic gene expression network is defective if cells are unable to properly express the different *GCR1* isoforms. Finally, when the levels of trehalose were assessed, it too was misregulated when either the nsDNA or the cDNA was expressed (Figure 4E), consistent with a role for the various *GCR1* isoforms in proper expression of products necessary for transition into different metabolic states.

Cells require both Gcr1 isoforms for proper growth and glycolytic gene expression

In light of the evidence that cells need to have the capacity to express both the spliced and unspliced *GCR1* isoforms for optimal growth and proper gene expression, we wanted to determine if coexpression of cDNA and nsDNA in *gcr1*Δ cells would imitate the condition of expressing gDNA. Both nsDNA and cDNA were coexpressed in *gcr1*Δ cells, which was compared with *gcr1*Δ cells expressing gDNA. *gcr1*Δ cells expressing both isoforms result in growth that is nearly indistinguishable from the expression of gDNA (Figure 5A). This is in stark contrast with sole expression of either of the individual isoforms (Figure 4) and indicates that cells require both isoforms for proper growth.

The fact that expression of both isoforms restores growth of *gcr1*Δ cells to levels equivalent to gDNA prompted us to determine how expression of the two isoforms affects gene expression. Consistent with growth, the glycolytic genes show a comparable level of expression relative to gDNA at the 2-, 4- and 6-hr timepoints upon expression of both isoforms (Figure 5B). Interestingly, at the 6-hr timepoint, there is a slight deregulation of *GDB1* and *GLC3*, which are involved in storage carbohydrate metabolism. This suggests to us that WT expression of genes involved in the process of breaking down glycogen may depend on the ratios of the Gcr1 isoforms that specifically arise from splicing. Nonetheless, the fact that these cells grow nearly identically to gDNA expressing cells indicates that growth, diauxic shift, and transition to stationary phase are not affected by these modest differences.

Gcr1 protein isoforms decrease post-diauxic shift

As the expression of both isoforms in *gcr1*Δ cells complement growth and gene expression to levels comparable to gDNA, we next wanted to determine how the Gcr1 protein isoforms change over time. As indicated in Figure 1, the interpretation of these results is confounded by the fact that the two proteins migrate with such similar mobilities. Moreover, phosphorylation of Gcr1 could mitigate distinct separation of two Gcr1 isoforms (Zeng et al., 1997). Hence, the strain in which each isoform has a different tag (Figures 5A and B) is particularly useful to assess isoform change over time. As we observed with the protein expressed from the endogenous *GCR1* (Figure 1A), the protein levels decrease rapidly at the 8-hr timepoint, as cells grow post diauxic shift. Interestingly, the nsDNA levels decrease sooner than the cDNA post-diauxic shift, similar to the pattern observed with the RNA (Figure 2B). For example, at 10 hrs compared to 2 hrs, the protein derived from nsDNA is nearly undetectable (Figure 5C). Meanwhile, the cDNA-derived protein is clearly still detectable albeit significantly decreased from earlier timepoints (Figure 5C). We observe similar results when the tags are reversed (data not shown). These data suggest that both the presence and the ratios of the Gcr1 isoforms are regulated by cells as they adjust to a changing metabolic environment.

Gcr1p isoforms form homo- and heterodimeric protein complexes

The growth and gene expression analyses reveal that cells with both isoforms are able to properly express the genes necessary for optimal growth in the presence of glucose. We considered the possibility that the proteins might interact with each other since previous studies suggested that Gcr1p forms a homodimer (Deminoff and Santangelo, 2001). To

address this, we performed co-immunoprecipitation (Co-IP) experiments using cells expressing the Gcr1p isoforms with different tags. To verify the efficiency of the immunoprecipitation and be sure that there was no cross reactivity of the antibodies to the different tags, we performed the co-IP experiments with lysates from *gcr1*Δ cells expressing nsDNA-TAP or nsDNA-myc using the anti-TAP antibody (Figure 6A). We efficiently immunoprecipitate TAP-tagged protein (Figure 6A, lane 2) using anti-TAP antibody, while it did not interact with the myc-tagged protein (Figure 6A, lane 4).

Next, we performed immunoprecipitation (IP) experiments using cell lysates from *gcr1*Δ cells co-expressing cDNA-TAP and nsDNA-myc. IP of the *GCR1* cDNA-derived protein with the TAP-specific antibody coimmunoprecipitated Gcr1 derived from the nsDNA (Figure 6B, lane 2), demonstrating the formation of a heterodimer between the proteins. We also carried out IPs from cells expressing both TAP and myc-tagged nsDNA to examine homodimer formation. IP with the anti-TAP antibody pulled down the myc-tagged protein (Figure 6B, lane 4) demonstrating that Gcr1 derived from the nsDNA can form a homodimer. Similar experiments were performed to examine homodimer formation between proteins derived from cDNA; IP of cDNA-TAP coimmunoprecipitated the cDNA-myc protein (Figure 6C, lane 2). Finally, we confirmed heterodimer formation by switching the tags between nsDNA and cDNA and pulling down nsDNA-TAP (Figure 6C, lane 4).

Taken together these results lead to a model in which alternative splicing plays a critical role in the cell's ability to adjust its metabolic needs (Figure 6D). As cells enter stationary phase, Gcr1 protein and RNA are downregulated. However, the transition from growth in high glucose requires a protein product generated from the removal of intron as well as a protein derived from a *GCR1* isoform in which the intron is retained. The finding that the Gcr1 protein actually can generate at least three different dimers (and possibly more if it interacts with other transcription factors, as has been proposed (Mizuno et al., 2004)) allows for a remarkable diversity in transcription factor activities as cells rapidly adjust their gene expression program to adapt to environmental changes.

Discussion

Here, we describe the discovery that the *GCR1* gene generates multiple protein isoforms, which are downregulated differentially upon glucose depletion. The Gcr1p isoforms physically interact and have different effects on glycolytic gene expression. This fine-tuned expression of Gcr1 is dependent upon alternative splicing of *GCR1*, particularly intron retention, and a surprising use of intronic translation initiation signals. *GCR1* regulation serves as an elegant example of how the convergence of multiple modes of gene regulation allows cells to respond to their environment and exert systems level control of gene expression.

Inefficient splicing and regulated degradation contribute to temporally regulated levels of alternative *GCR1* transcripts

Although relatively few yeast genes contain multiple introns, there is a growing appreciation for the role that non-consensus splice sites play in regulated intron-retention in yeast (see review by (Johnson and Vilardell, 2012)). For example, we recently showed that the *SUS1*

intron is retained, particularly under specific stress conditions (Hossain et al., 2011), and it appears that a small peptide may be generated from this transcript (Cuenca-Bono et al., 2011). Here we show that *GCR1* expression is also regulated at the level of intron retention, most likely due to non-consensus splice sites present in the intron.

One of the unexpected observations is that *GCR1* levels are heavily regulated by cytoplasmic decay machinery, particularly Xrn1. Surprisingly, deletion of Upf1 has a relatively small effect on the levels of the *GCR1* isoforms (Figure 2E). These data suggest that *GCR1* is co-localized with Xrn1, perhaps in processing bodies (Sheth and Parker, 2003; Teixeira et al., 2005) to facilitate rapid reintroduction into the RNA pool for translation when cellular conditions are appropriate.

GCR1 reveals an unexpected mode of translational regulation

A recent survey of alternative translation used comparative genomics to demonstrate that alternative start sites within single transcripts are under negative selection across species (Bazykin and Kochetov, 2011). However, genes involved in transcriptional regulation are significantly overrepresented among genes with conserved downstream AUGs (Bazykin and Kochetov, 2011). A recently described example of this is the mammalian PTPB3 gene, which generates different protein isoforms by alternative translation initiation as a result of re-initiation of translation and leaky ribosome scanning (Tan et al., 2015). It is possible that highly-conserved AUGs within the *GCR1* intron are used by the translation machinery by a similar mechanism. Nonetheless, to our knowledge this is the first example of an alternative protein isoform generated from in-frame translation initiation within an annotated intron.

The *GCR1* gene generates an RNA that encodes the second exon

GCR1 generates an alternative transcript with its 5′ end near the beginning of Exon2. Although there is no obvious sequence defining this as a transcription start site (TSS), there is a putative Gcr1 binding site (CTTCC) in the intron that lies just upstream of the branchpoint that may be responsible for the expression of this RNA. While it is not unusual for there to be multiple TSSs that influence protein production within a single 5′UTR in yeast (Rojas-Duran and Gilbert, 2012), the presence of an alternative TSS at the exon and possible regulatory sequences within the intron is surprising. In mammals, alternative TSSs are believed to contribute to more mRNA isoforms than alternative splicing in some tissues (Pal et al., 2011). Our data suggest that *GCR1* also may have similarly evolved to permit simultaneous transcription from multiple TSSs under particular conditions in yeast. While we do not find convincing evidence that a protein is produced from this small RNA, we note that an in-frame peptide could be produced from this RNA comprising the entire DNA binding domain. Alternatively, expression of a noncoding RNA could affect transcription of the full length *GCR1* transcript, which we are also exploring.

Gcr1 isoforms are required for systems level control of glycolytic gene expression

The complex network of glycolytic gene expression is controlled by the concerted action of multiple transcription factors. For example, *in vivo* mapping of binding sites of these regulatory factors reveals that for several Gcr1-regulated genes, the Gcr1 binding sites are located adjacent to the Rap1, Abf1 and Reb1 binding sites (Scott and Baker, 1993) (Willett

et al., 1993). By existing in multiple isoforms, forming dimers, and interacting in close proximity to other transcription factors, Gcr1 regulation allows dynamic fine-tuning of glycolytic genes expression, which we show is dependent on the presence of both isoforms (Figure 4).

The precise determinants of transcriptional regulation and splicing efficiency in response to metabolic changes remain to be fully elucidated. Interestingly, Cbp80, the large subunit of the cap-binding complex in yeast (yCBC), was originally identified as Gcr3 in a screen for mutants with reduced glycolytic enzyme expression (Uemura and Jigami, 1992). The yCBC has also been implicated in transcriptional regulation (Hossain et al., 2013; Lahudkar et al., 2011), splicing fidelity, particularly at the 5′SS (Hossain et al., 2009), and the coordination of splicing and transcription (Bragulat et al., 2010; Gornemann et al., 2005). Intriguingly, we have found that CBC expression also changes in response to glucose availability (data not shown), suggesting that the CBC might play a critical role in regulating Gcr1 expression in response to glucose, a model we are currently testing. In conclusion, understanding how Gcr1 is regulated and the role of this regulation in metabolic responses provides exciting insights into cellular adaptability in a changing environment.

Experimental Procedures

Yeast strains and growing culture

All strains are derived from BY4742 and individual deletion strains were obtained from Open Biosystems (Table S2). Yeast strains were grown in standard YP media supplemented with dextrose to a final concentration of 2% (YPD) at 30°C. For timepoints, overnight cultures were diluted to an OD_{600} of ~ 0.1 in 100ml YPD. Cultures were harvested at 0.3 OD_{600}, precipitated and then resuspended in 100ml of fresh YPD. Timepoints were taken at 2 hr intervals (0 hr is 0.3 OD_{600}). At each timepoint, $O.D_{600}$ was measured and 10ml of cells were precipitated, flash frozen and stored at −80°C. For the complementation assay, *gcr1*Δ cells were cotransformed with plasmids pRS315-gDNA + pRS313, pRS315-nsDNA + pRS313-cDNA or pRS315-cDNA + pRS313-nsDNA. Transformants were grown in SC-his-leu. Growth was measured as described above.

Preparation *GCR1* constructs

GCR1 constructs were generated by standard PCR methods using the primers listed in Table S1. Each clone was verified by sequencing before use (See supplemental experimental procedures).

Western blot analysis

For western blot analysis, equal amounts of protein extracted from the appropriate timepoint was fractionated by gel electrophoresis, and the blots were probed with the appropriate antibody. Equal loading was also determined by SDS-PAGE gels and use of a loading control (See supplemental experimental procedures).

Northern blot analysis

RNA was isolated from cell pellets collected at each time point using hot phenol. An equal amount of total RNA (~30μg) was separated by denaturing agarose-formaldehyde gel electrophoresis and transferred to Zeta probe membrane (Bio-Rad). The membrane was hybridized with radio-labeled probes specific to *GCR1*. The lower part of membrane was cut and probed with radiolabeled *SCR1*. For probe walking northern experiments, see supplemental experimental procedures.

RT-PCR and real time PCR analysis

RNA was isolated from cells at indicated time points, and then cDNA was synthesized. RT-PCR products were analyzed in polyacrylamide gels and stained with SYBR green. Real-time PCR was performed from the diluted cDNA and quantitation was performed by $2^{\Delta ct}$ or $2^{\Delta\Delta ct}$ methodology (See supplemental experimental procedures).

Co-immunoprecipitation and western blot analysis

Cell lysates were extracted from *gcr1*Δ cells expressing both nsDNA and cDNA isoforms containing different tags. Co-immunoprecipitations were carried out using anti-TAP antibody. Eluted protein was then detected by western blot using anti-TAP and anti-myc antibody (See supplemental experimental procedures).

Supplementary Material

Refer to Web version on PubMed Central for supplementary material.

Acknowledgments

This work was supported by the National Science Foundation (MCB-1051921 to T.L.J.), and the National Institute of General Medical Sciences (GM-079333 to J.H. and T.L.J. and GM-085474 to T.L.J.). This work was also supported by a Ruth L. Kirschstein National Research Service Award GM-007185 supporting S.E.

References

Bazykin GA, Kochetov AV. Alternative translation start sites are conserved in eukaryotic genomes. Nucleic Acids Res. 2011; 39:567–577. [PubMed: 20864444]

Bon E, Casaregola S, Blandin G, Llorente B, Neuveglise C, Munsterkotter M, Guldener U, Mewes HW, Van Helden J, Dujon B, et al. Molecular evolution of eukaryotic genomes: hemiascomycetous yeast spliceosomal introns. Nucleic Acids Res. 2003; 31:1121–1135. [PubMed: 12582231]

Bragulat M, Meyer M, Macias S, Camats M, Labrador M, Vilardell J. RPL30 regulation of splicing reveals distinct roles for Cbp80 in U1 and U2 snRNP cotranscriptional recruitment. RNA. 2010; 16:2033–2041. [PubMed: 20801768]

Chambers A, Packham EA, Graham IR. Control of glycolytic gene expression in the budding yeast (Saccharomyces cerevisiae). Curr Genet. 1995; 29:1–9. [PubMed: 8595651]

Cuenca-Bono B, Garcia-Molinero V, Pascual-Garcia P, Dopazo H, Llopis A, Vilardell J, Rodriguez-Navarro S. SUS1 introns are required for efficient mRNA nuclear export in yeast. Nucleic Acids Res. 2011

Deminoff SJ, Santangelo GM. Rap1p requires Gcr1p and Gcr2p homodimers to activate ribosomal protein and glycolytic genes, respectively. Genetics. 2001; 158:133–143. [PubMed: 11333224]

DeRisi JL, Iyer VR, Brown PO. Exploring the metabolic and genetic control of gene expression on a genomic scale. Science. 1997; 278:680–686. [PubMed: 9381177]

Gasch AP, Spellman PT, Kao CM, Carmel-Harel O, Eisen MB, Storz G, Botstein D, Brown PO. Genomic expression programs in the response of yeast cells to environmental changes. Mol Biol Cell. 2000; 11:4241–4257. [PubMed: 11102521]

Gornemann J, Kotovic KM, Hujer K, Neugebauer KM. Cotranscriptional spliceosome assembly occurs in a stepwise fashion and requires the cap binding complex. Mol Cell. 2005; 19:53–63. [PubMed: 15989964]

Gray JV, Petsko GA, Johnston GC, Ringe D, Singer RA, Werner-Washburne M. “Sleeping beauty”: quiescence in Saccharomyces cerevisiae. Microbiol Mol Biol Rev. 2004; 68:187–206. [PubMed: 15187181]

Hossain MA, Chung C, Pradhan SK, Johnson TL. The yeast cap binding complex modulates transcription factor recruitment and establishes proper histone H3K36 trimethylation during active transcription. Mol Cell Biol. 2013; 33:785–799. [PubMed: 23230273]

Hossain MA, Claggett JM, Nguyen T, Johnson TL. The cap binding complex influences H2B ubiquitination by facilitating splicing of the SUS1 pre-mRNA. Rna. 2009; 15:1515–1527. [PubMed: 19561118]

Hossain MA, Rodriguez CM, Johnson TL. Key features of the two-intron Saccharomyces cerevisiae gene SUS1 contribute to its alternative splicing. Nucleic Acids Res. 2011

Huie MA, Scott EW, Drazinic CM, Lopez MC, Hornstra IK, Yang TP, Baker HV. Characterization of the DNA-binding activity of GCR1: in vivo evidence for two GCR1-binding sites in the upstream activating sequence of TPI of Saccharomyces cerevisiae. Mol Cell Biol. 1992; 12:2690–2700. [PubMed: 1588965]

Johnson TL, Vilardell J. Regulated pre-mRNA splicing: the ghostwriter of the eukaryotic genome. Biochimica et biophysica acta. 2012; 1819:538–545. [PubMed: 22248620]

Kawashima T, Douglass S, Gabunilas J, Pellegrini M, Chanfreau GF. Widespread use of non-productive alternative splice sites in Saccharomyces cerevisiae. PLoS Genet. 2014; 10:e1004249. [PubMed: 24722551]

Lahudkar S, Shukla A, Bajwa P, Durairaj G, Stanojevic N, Bhaumik SR. The mRNA cap-binding complex stimulates the formation of pre-initiation complex at the promoter via its interaction with Mot1p in vivo. Nucleic Acids Res. 2011; 39:2188–2209. [PubMed: 21075799]

Longo VD, Fabrizio P. Regulation of longevity and stress resistance: a molecular strategy conserved from yeast to humans? Cell Mol Life Sci. 2002; 59:903–908. [PubMed: 12169020]

Lopez MC, Baker HV. Understanding the growth phenotype of the yeast gcr1 mutant in terms of global genomic expression patterns. J Bacteriol. 2000; 182:4970–4978. [PubMed: 10940042]

Mizuno T, Kishimoto T, Shinzato T, Haw R, Chambers A, Wood J, Sinclair D, Uemura H. Role of the N-terminal region of Rap1p in the transcriptional activation of glycolytic genes in Saccharomyces cerevisiae. Yeast. 2004; 21:851–866. [PubMed: 15300680]

Pal S, Gupta R, Kim H, Wickramasinghe P, Baubet V, Showe LC, Dahmane N, Davuluri RV. Alternative transcription exceeds alternative splicing in generating the transcriptome diversity of cerebellar development. Genome Res. 2011; 21:1260–1272. [PubMed: 21712398]

Rojas-Duran MF, Gilbert WV. Alternative transcription start site selection leads to large differences in translation activity in yeast. RNA. 2012; 18:2299–2305. [PubMed: 23105001]

Sasaki H, Uemura H. Influence of low glycolytic activities in gcr1 and gcr2 mutants on the expression of other metabolic pathway genes in Saccharomyces cerevisiae. Yeast. 2005; 22:111–127. [PubMed: 15645478]

Sayani S, Janis M, Lee CY, Toesca I, Chanfreau GF. Widespread impact of nonsense-mediated mRNA decay on the yeast intronome. Molecular cell. 2008; 31:360–370. [PubMed: 18691968]

Scott EW, Baker HV. Concerted action of the transcriptional activators REB1, RAP1, and GCR1 in the high-level expression of the glycolytic gene TPI. Mol Cell Biol. 1993; 13:543–550. [PubMed: 8417350]

Shah KH, Zhang B, Ramachandran V, Herman PK. Processing body and stress granule assembly occur by independent and differentially regulated pathways in Saccharomyces cerevisiae. Genetics. 2013; 193:109–123. [PubMed: 23105015]

Sheth U, Parker R. Decapping and decay of messenger RNA occur in cytoplasmic processing bodies. Science. 2003; 300:805–808. [PubMed: 12730603]

Tan LY, Whitfield P, Llorian M, Monzon-Casanova E, Diaz-Munoz MD, Turner M, Smith CW. Generation of functionally distinct isoforms of PTBP3 by alternative splicing and translation initiation. Nucleic Acids Res. 2015; 43:5586–5600. [PubMed: 25940628]

Teixeira D, Sheth U, Valencia-Sanchez MA, Brengues M, Parker R. Processing bodies require RNA for assembly and contain nontranslating mRNAs. RNA. 2005; 11:371–382. [PubMed: 15703442]

Tornow J, Santangelo G. The GCR1 gene of Saccharomyces cerevisiae is a split gene with an unusually long intron. Genetics. 1994; 138:973–974. [PubMed: 7851789]

Tornow J, Zeng X, Gao W, Santangelo GM. GCR1, a transcriptional activator in Saccharomyces cerevisiae, complexes with RAP1 and can function without its DNA binding domain. EMBO J. 1993; 12:2431–2437. [PubMed: 8508768]

Uemura H, Fraenkel DG. gcr2, a new mutation affecting glycolytic gene expression in Saccharomyces cerevisiae. Mol Cell Biol. 1990; 10:6389–6396. [PubMed: 2247062]

Uemura H, Jigami Y. GCR3 encodes an acidic protein that is required for expression of glycolytic genes in Saccharomyces cerevisiae. J Bacteriol. 1992; 174:5526–5532. [PubMed: 1512188]

Warner JR. The economics of ribosome biosynthesis in yeast. Trends Biochem Sci. 1999; 24:437–440. [PubMed: 10542411]

Willett CE, Gelfman CM, Holland MJ. A complex regulatory element from the yeast gene ENO2 modulates GCR1-dependent transcriptional activation. Mol Cell Biol. 1993; 13:2623–2633. [PubMed: 8455635]

Yoshikawa K, Tanaka T, Ida Y, Furusawa C, Hirasawa T, Shimizu H. Comprehensive phenotypic analysis of single-gene deletion and overexpression strains of Saccharomyces cerevisiae. Yeast. 2011; 28:349–361. [PubMed: 21341307]

Zeng X, Deminoff SJ, Santangelo GM. Specialized Rap1p/Gcr1p transcriptional activation through Gcr1p DNA contacts requires Gcr2p, as does hyperphosphorylation of Gcr1p. Genetics. 1997; 147:493–505. [PubMed: 9335588]

Highlights

- *GCR1* generates multiple isoforms under glucose-rich conditions
- Intron-retention supports translation of a critical Gcr1 isoform from intronic AUGs
- The Gcr1p isoforms derived from spliced and unspliced *GCR1* form dimers
- The Gcr1 isoforms are necessary for proper, temporally-regulated gene expression

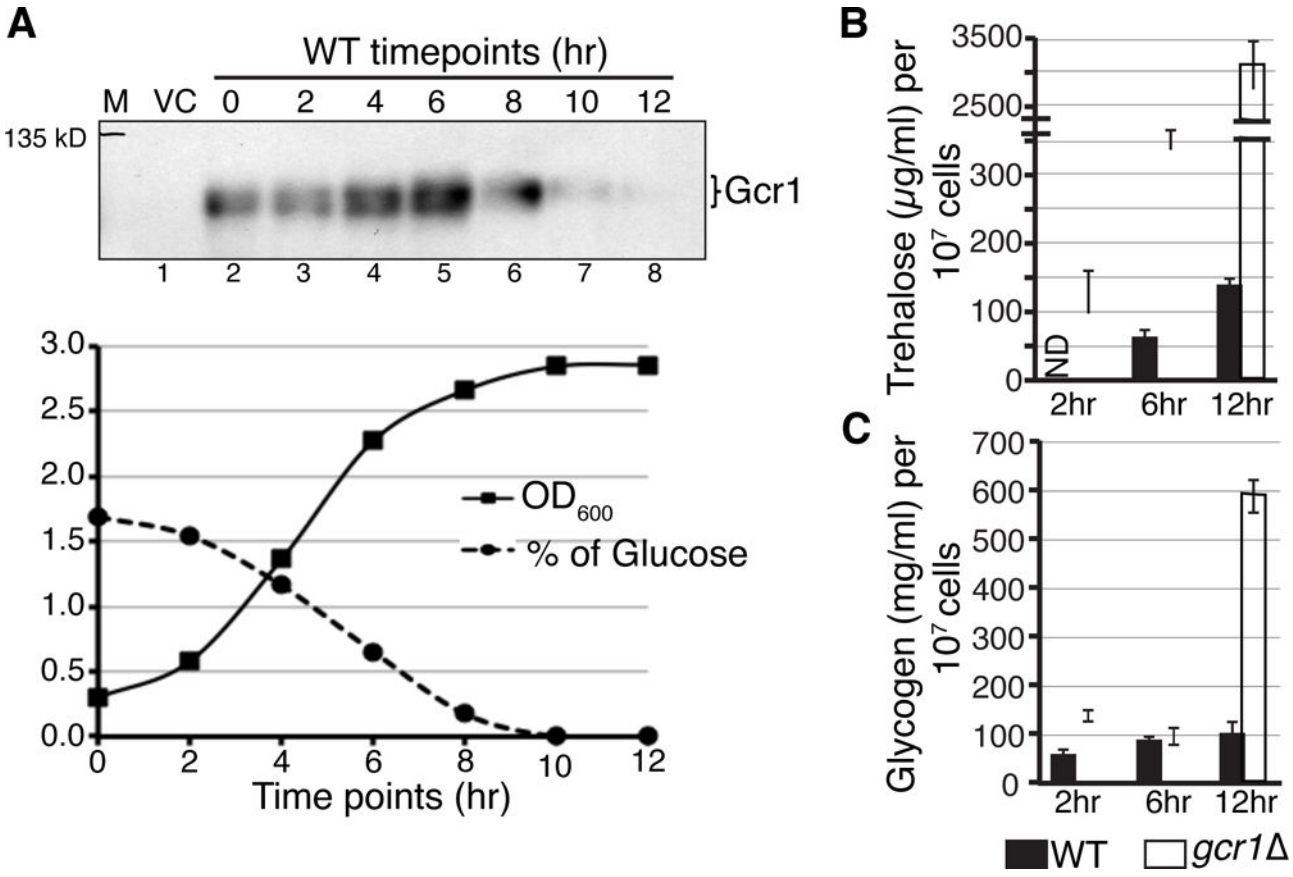

Figure 1. Gcr1p expression is regulated in response to glucose and deletion of *GCR1* leads to premature accumulation of storage carbohydrates

(A) Western blot analysis showing Gcr1p levels at indicated timepoints when cells were grown in media containing glucose. The bottom panel shows the corresponding growth curve, including an analysis of extracellular glucose concentration at the timepoints indicated. (B) Trehalose and (C) glycogen levels were analyzed for WT and *gcr1*Δ cells collected at the indicated timepoints. ND= not detectable. See also figure S1.

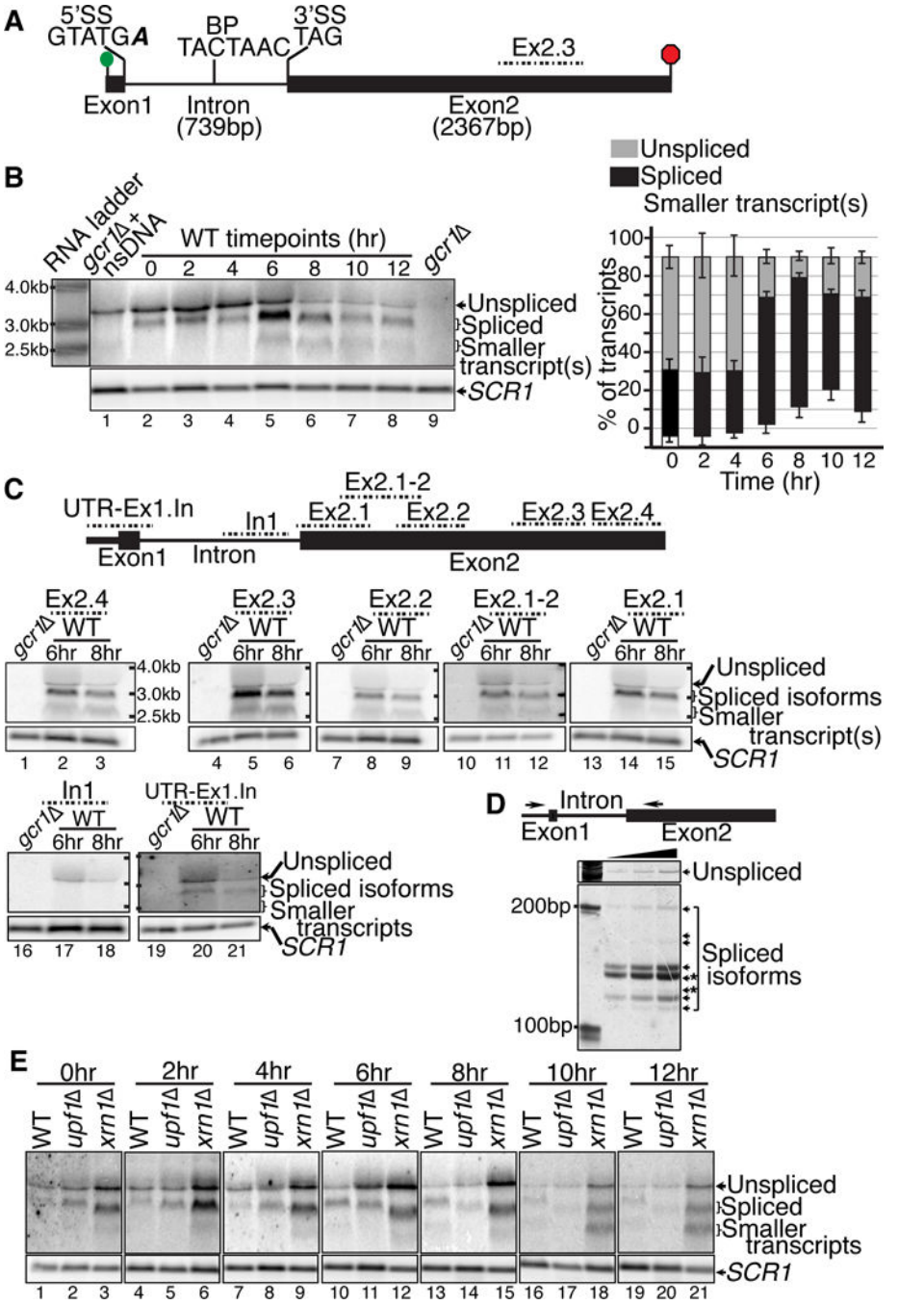

Figure 2. Splicing of *GCR1* changes in response to glucose. *GCR1* undergoes alternative splicing to generate multiple isoforms that are subjected to decay

(A) Schematic of *GCR1* highlighting the intron (black line), exons (black boxes) and splice sites of the intron. The dotted line above Exon2 indicates the region corresponding to the northern probe Ex2.3. The green circle indicates the start codon ATG and red circle indicates the stop codon. (B) Northern analysis showing the hybridization of unspliced, spliced isoforms, and the smaller transcript(s) with a probe specific to *GCR1*. The lower panel shows *SCR1* as a loading control. The bar graph shows a quantitative analysis of the relative levels of each *GCR1* transcript at indicated time points. Each bar represents the average

±SEM, n=3 (C) Northern blot (probe walking) experiments to determine the identity of RNAs. Multiple sets of *gcr1*Δ, 6 hr, 8 hr RNA samples were run on a northern gel separated by a RNA ladders. Then the membranes were cut into strips through the markers. Probes corresponding to different regions of *GCR1* were hybridized separately to each set of samples. Dotted lines on the *GCR1* schematic show the region and name of the northern probes. RNA ladders are indicated for each blot by short black lines. *SCR1* serves as the loading control. For A–C, see also figure S2. (D) RT-PCR followed by DNA PAGE analysis shows that alternative splicing of *GCR1* generates multiple isoforms. Primers are indicated by arrows on the schematic of *GCR1.* Asterisks indicate isoforms that contain a translational ATG in frame with the stop codon. See also figure S3. (E) *GCR1* transcripts are subjected to cytoplasmic decay. Blots were probed with the Ex2.3 probe shown in figure 2C. *SCR1* serves as the loading control. See also figure S4.

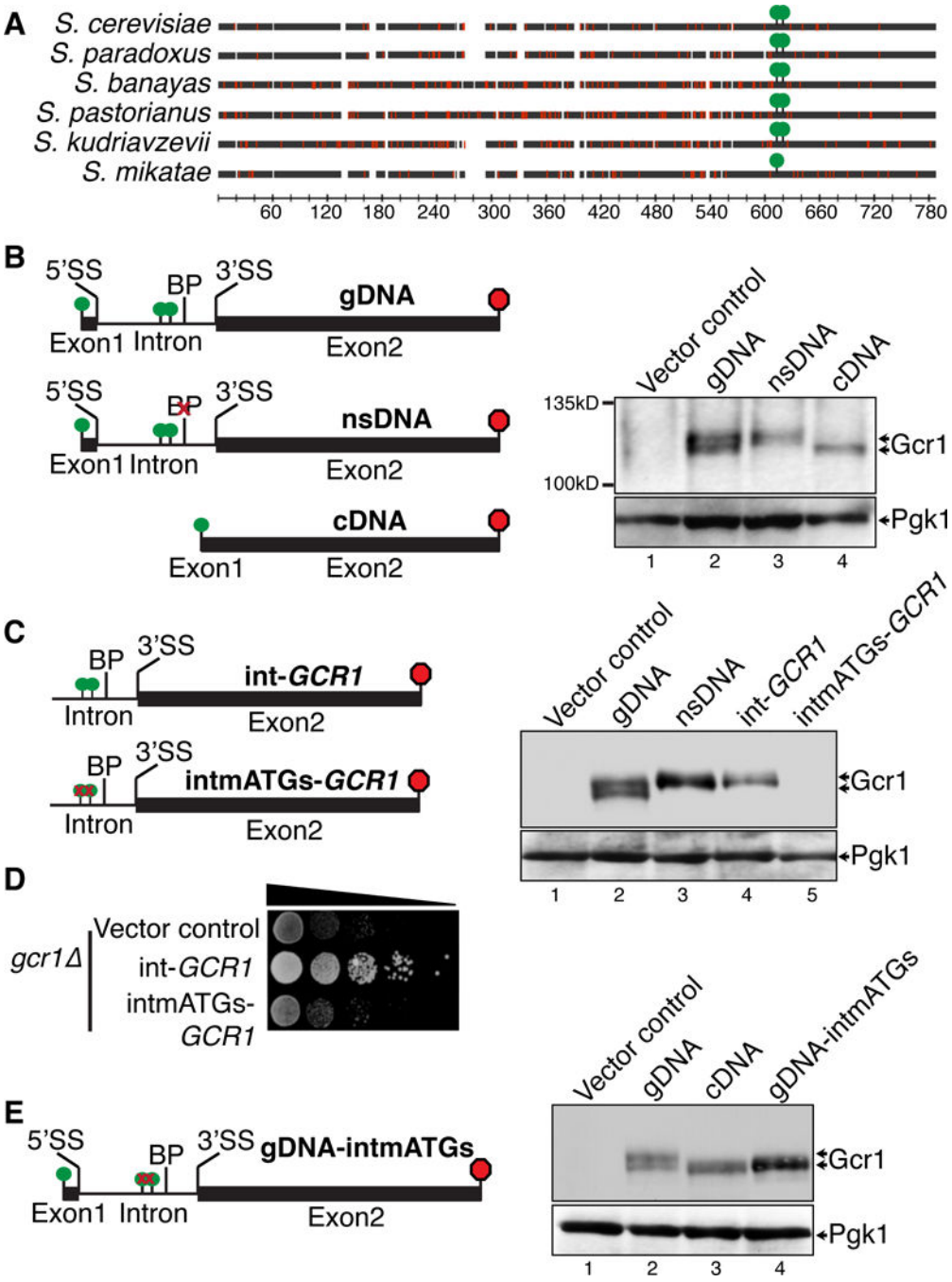

Figure 3. *GCR1* produces two proteins, one encoded by the spliced isoform (cDNA) and the other encoded by the unspliced isoform (nsDNA)

(A) Schematic representation of the intron sequence alignment among the *Saccharomyces* sp. The black bars indicate conserved sequences within the intron. The white bars indicate sequence gaps and red lines represent non-conserved bases among the sequences. The green circles indicate the highly conserved intronic ATG, which is in translational frame with the *GCR1* stop codon. (B) Schematics show the expression constructs gDNA, nsDNA and cDNA. In the nsDNA construct, red (X) indicates the mutation of the branchpoint sequence. The green circles indicate the ATGs. The red circle at the end of Exon2 shows the stop

codon. Western blot analysis shows the expression of Gcr1p from gDNA, nsDNA and cDNA constructs. The mobility of a molecular wt. marker is indicated to the left side of the gel. Pgk1 serves as a loading control. See also figure S5A. (C) The schematic shows the expression construct int-*GCR1*, which contains the intronic ATG and upstream sequences, but not Exon1. In the intmATGs-*GCR1* construct, the intronic ATGs were mutated (red X). Western blot analysis shows the expression and migration of Gcr1p from gDNA, nsDNA, int-*GCR1* and intmATGs-*GCR1*. (D) The growth analysis experiment shows that int-*GCR1* expression rescues the growth defect of *gcr1*Δ while expression of intmATGs-*GCR1* shows no effect on the growth of *gcr1*Δ. See also figure S5B. (E) The schematic shows the gDNA-intmATGs construct, in which the intronic ATGs were mutated. Western blot analysis was performed to analyze the expression and migration of Gcr1p. All the Western blots were performed with cell lysates extracted from cells at 2 hr timepoints. Pgk1 serves as the loading control. See also figure S5.

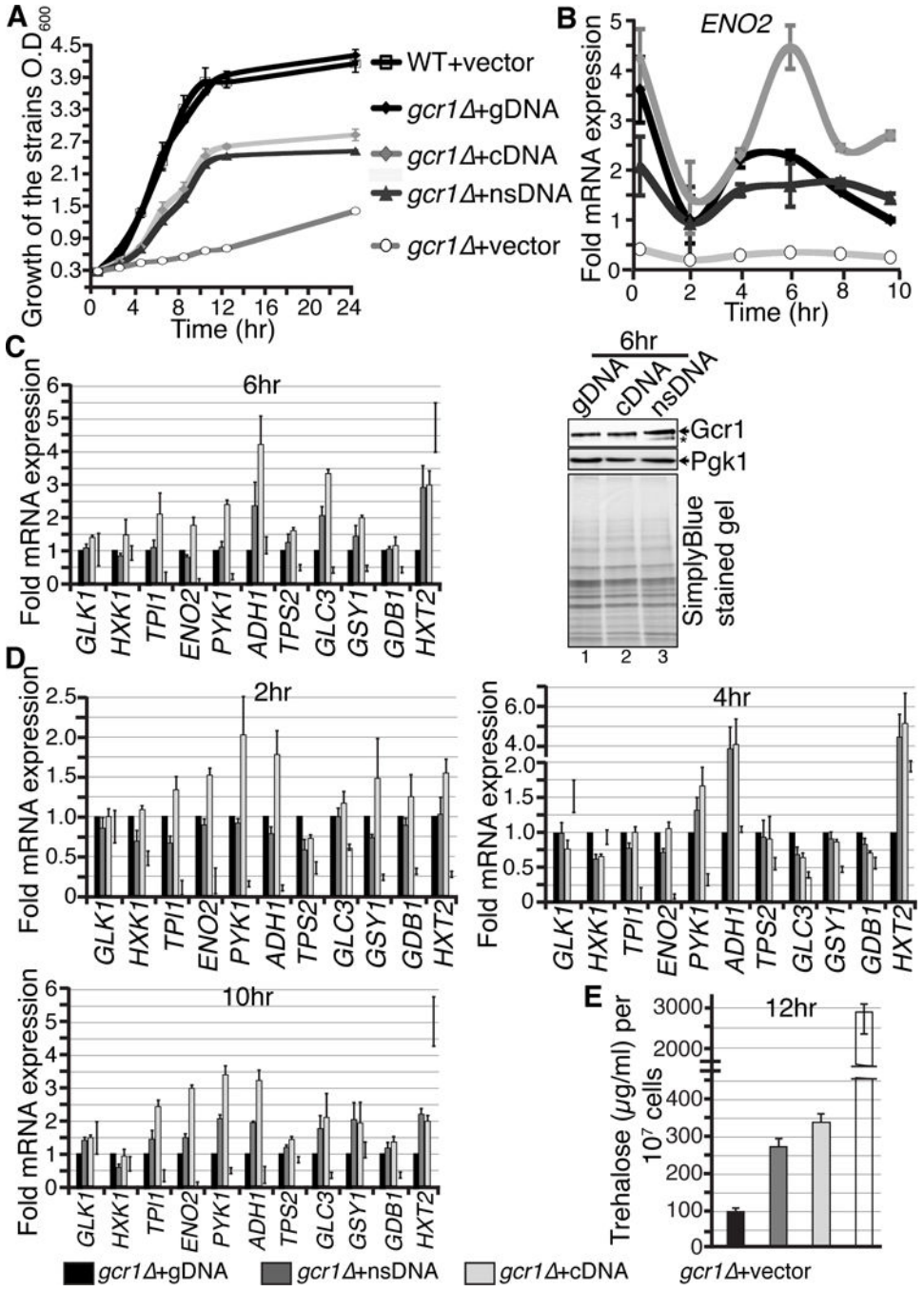

Figure 4. Cells expressing only one isoform of Gcr1p display growth defects and variability in glycolytic gene expression

(A) Ectopic expression of cDNA or nsDNA alone in *gcr1*Δ cells results in a growth defect compared to the cells expressing gDNA. Line graph shows the average of three independent experiments with SEM. (B) The line graph shows expression of the *ENO2* gene in *gcr1*Δ cells expressing gDNA, nsDNA, cDNA or empty vector. Fold expression was analyzed by ΔC_t method compared to *SCR1*. Values are presented as average±SEM (n=3). (C) Shows the variable expression of genes involved in glucose metabolism. Fold gene expression was analyzed in *gcr1*Δ+nsDNA, *gcr1*Δ+cDNA and *gcr1*Δ+vector cells by $2^{-\Delta\Delta C_t}$ method

compared to *SCR1* and then normalized to the expression of *gcr1*Δ+gDNA. The bar graph represents the average of three biological replicates with SEM. Western blots show the level of Gcr1p expressing from gDNA, cDNA and nsDNA at 6hr timepoint. Pgk1 serves as the loading control. Asterisks indicate the non-specific band. SimplyBlue stained SDS-PAGE shows the equivalent amount of total protein loaded for western blot from each sample. (D) Gene expression analysis shows variable expression of genes involved in glucose metabolism at 2 hr, 4 hr and 10 hr timepoints. Fold gene expression was analyzed as described above. The bar graphs represent the average±SEM (n=3). See also figure S6. (E) Trehalose accumulation in the indicated cells at the 12 hr timepoint.

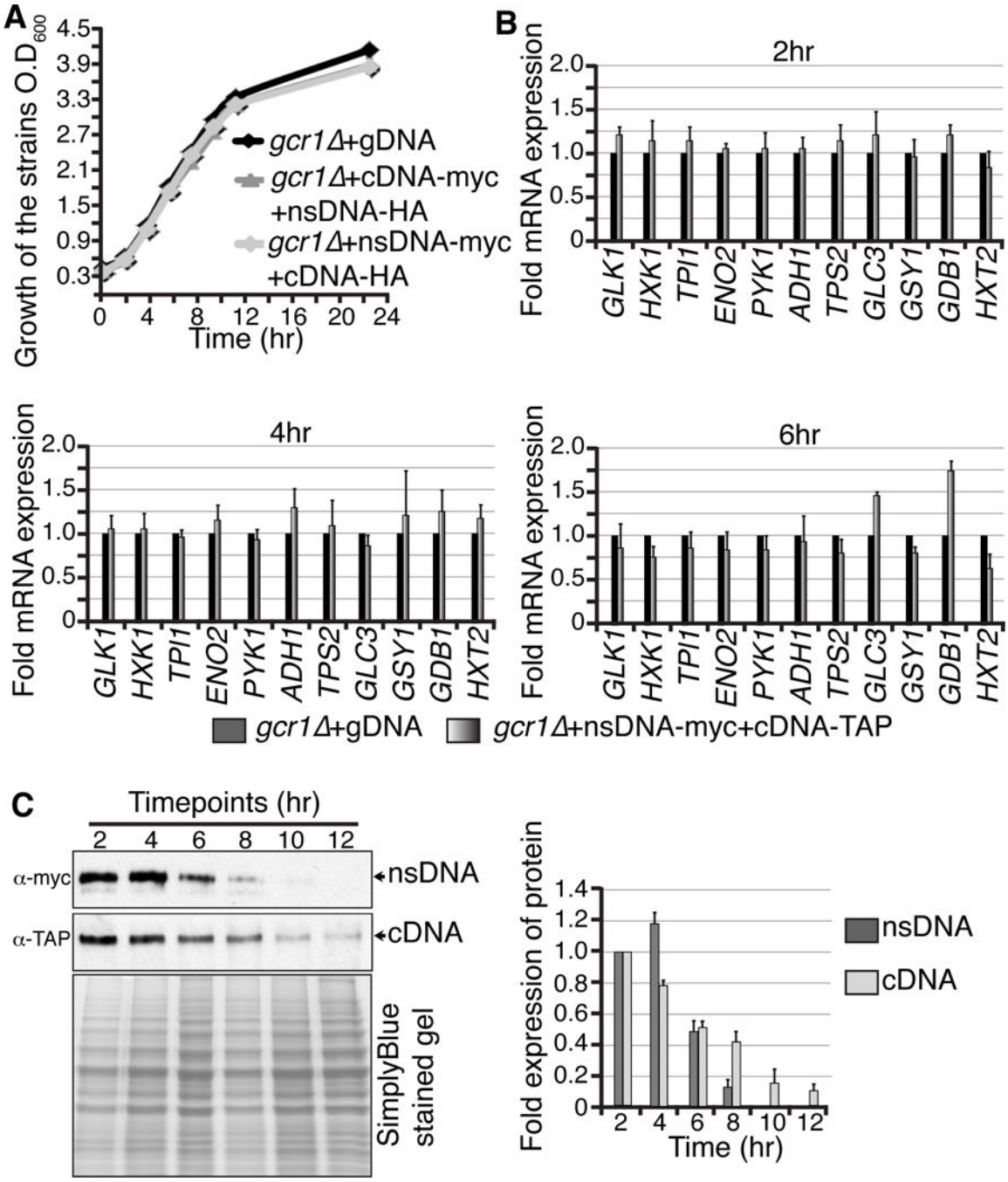

Figure 5. Cells require both isoforms of Gcr1p for optimal growth and proper glycolytic gene expression

(A) Growth analysis comparing growth of *gcr1*Δ cells expressing gDNA to cells coexpressing nsDNA and cDNA (where n= at least 3 with SEM). (B) Gene expression analysis shows the expression of glycolytic genes in *gcr1*Δ+nsDNA+cDNA compared to expression of gDNA at the 2-, 4- and 6 hr timepoints. Fold expression was analyzed by $\Delta\Delta C_t$ as described in figure 4C. Bar graphs represent the average with SEM, where n=3. (C) Western blot analysis showing the levels of protein from the nsDNA and cDNA constructs from the same cell lysates at the indicated timepoints. The antibody used for detection is

indicated at the left side of the blots. The lower panel is simplyBlue-stained gel to show the total protein from each time point. The bar graph shows the fold expression of protein over time (Average± SD, where n=2).

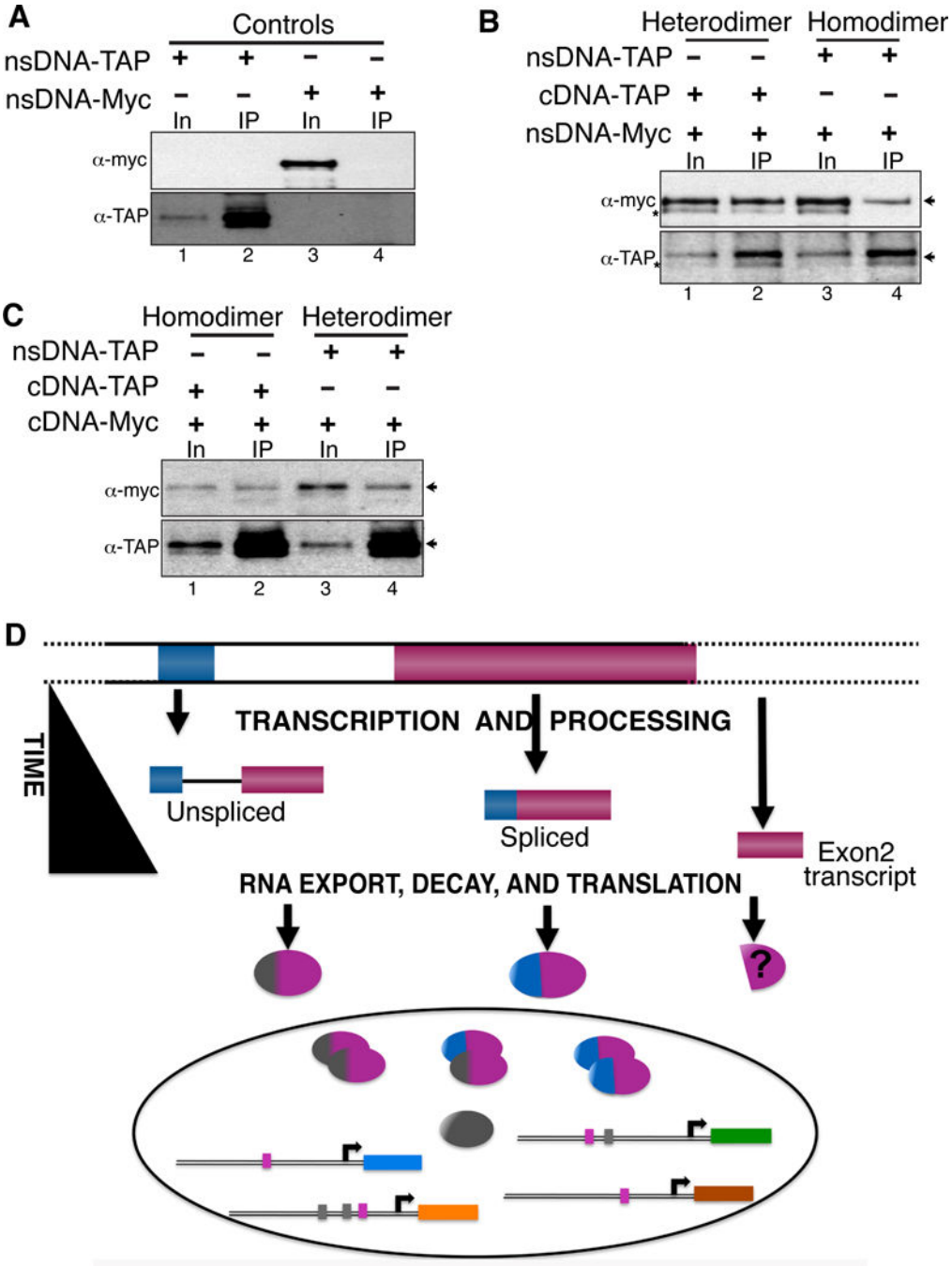

Figure 6. Protein isoforms generated from *GCR1* cDNA and nsDNA make Gcr1 homodimer and heterodimer

(A) nsDNA-TAP (lanes 1 and 2, lower blot) protein is efficiently immunoprecipitated with anti-TAP antibody. Gcr1-TAP does not cross react with anti-myc antibody (lanes 1 and 2, upper blot). nsDNA-myc protein neither coimmunoprecitates (lane 4 upper blot) nor crossreacts with anti-TAP antibody (lanes 3 and 4 lower blot). (B) nsDNA-myc protein coprecipitates with cDNA-TAP (lanes 1 and 2) and nsDNA-TAP (lanes 3 and 4). Coimmunoprecipitation (Co-IP) experiments were performed using cell lysates co-expressing *GCR1* cDNA-TAP or *GCR1* nsDNA-TAP and *GCR1* nsDNA-myc. (C) cDNA-

myc protein coimmunoprecipitates with cDNA–TAP (lanes 1 and 2) and nsDNA-TAP (lanes 3 and 4). Co-IP experiments were performed from the cell lysates co-expressing *GCR1* cDNA-TAP or *GCR1* nsDNA-TAP and *GCR1* cDNA-myc Co-IPs were performed using anti-TAP antibody. Blots were probed with the indicated antibody.

(D) Model showing how alternative RNA processing leads to temporal expression of multiple Gcr1p isoforms to fine-tune glycolytic gene expression. The blue box represents the Exon1 and the purple box represents the Exon2. Gray/purple ovals represent the protein generated from the unspliced *GCR1* and the protein generated from cDNA is represented by the blue/purple oval. The bottom panel of the model depicts the possible cellular activities of the Gcr1p in order to regulate the gene expression of target genes. The gray oval represents other transcription factors that may contribute to regulation of Gcr1 responsive genes.